PHYSICAL REVIEW B **79**, 241311(R) (2009)

Origin of one-photon and two-photon optical transitions in PbSe nanocrystals

A. Franceschetti, J. W. Luo, J. M. An, and A. Zunger
National Renewable Energy Laboratory, Golden, Colorado 80401, USA
(Received 7 May 2009; published 17 June 2009)

PbSe nanocrystals represent the paradigm nanoscale system exhibiting carrier multiplication upon light absorption, yet their absorption spectrum is poorly understood. Two very different interpretations of the absorption peaks have been proposed: is the second absorption peak a *dipole-forbidden* S_h-P_e or P_h-S_e transition or a *dipole-allowed* P_h-P_e transition? A recent two-photon photoluminescence-excitation experiment favored the first interpretation, raising the question of why a dipole-forbidden transition would be strongly absorptive. Here we report atomistic pseudopotential calculations of the one-photon and two-photon absorption spectra of PbSe nanocrystals, showing unequivocally that, contrary to previous interpretations by other authors, the second one-photon absorption peak originates from dipole-allowed P_h-P_e transitions.

DOI: 10.1103/PhysRevB.79.241311 PACS number(s): 78.67.Bf, 78.40.Fy, 78.55.Qr

Nanostructures made of narrow-band-gap semiconductors, such as lead selenide (ε_{gap}=0.28 eV in bulk), have attracted considerable interest in recent years because of their potential applications as light absorbers in nanostructured solar-cell devices.[1] Efficient carrier multiplication, whereby two or more electron-hole pairs are generated by a single absorbed photon,[2,3] holds the promise[1] of dramatically exceeding the efficiency limit of single-junction solar cells. The ability to use PbSe nanocrystals (NCs) as light absorbers depends critically on a fundamental understanding of their absorption spectrum. Despite a number of experimental[2–16] and theoretical[3,17–27] studies, however, the origin of the absorption peaks remains a mystery.

The absorption spectrum of PbSe NCs typically shows three main peaks. There are currently two very different interpretations of the absorption peaks in terms of interband transitions. (1) In the first model [model I, depicted in Fig. 1(a)],[2–4,9–11,14,17,21] the three main absorption peaks are assigned to the (i) S_h-S_e, (ii) S_h-P_e and P_h-S_e, and (iii) P_h-P_e interband transitions, respectively. Here S and P denote the dominant angular-momentum character of the envelope functions, and the subscripts h and e refer to hole and electron wave functions. Most notably, model I assumes that the dipole-forbidden S_h-P_e and P_h-S_e transitions can be observed in one-photon linear absorption experiments. The mechanism that renders such dipole-forbidden transitions as experimentally intense has not been identified. This model has been used to interpret not only the interband absorption peaks but also other properties of PbSe NCs, such as the large photon-energy threshold for carrier multiplication[2] and the relatively slow intraband electron relaxation rate.[11] (2) In the second model [model II, depicted in Fig. 1(b)] (Refs. 6, 16, and 23) the three main absorption peaks are assigned to the (i) S_h-S_e, (ii) $P_h^{\parallel}$-$P_e^{\parallel}$, and (iii) a mixture of $P_h^{\perp}$-$P_e^{\perp}$ and D_h-D_e interband transitions, respectively. This model is based on the recognition that because the band-edge states of PbSe NCs are L-derived, not Γ-derived, the P-like NC states are split into separate $P^{\parallel}$ and $P^{\perp}$ manifolds.[23] An expansion of the NC states in terms of bulk Bloch states shows that the $P^{\parallel}$ states originate from $\boldsymbol{k}$ points located along the longitudinal direction of the L valleys in the bulk Brillouin zone, whereas $P^{\perp}$ states originate from $\boldsymbol{k}$ points in the perpendicular direction.[23] Because the longitudinal effective mass at the L point is larger than the perpendicular effective mass, $P_e^{\parallel}$ ($P_h^{\parallel}$) states have lower (higher) energy than $P_e^{\perp}$ ($P_h^{\perp}$) states.

The evidence in support of model I is based primarily on the agreement between the energy of the measured absorption peaks and the energy of the calculated S_h-S_e, S_h-P_e (or P_h-S_e), and P_h-P_e transitions. Such agreement was reported both in the case of effective-mass $\mathbf{k}\cdot\mathbf{p}$ calculations[3,17,21] and in the case of atomistic tight-binding calculations.[14,20] As pointed out in Ref. 23, however, the effective-mass calculations of Refs. 3, 17, and 21 do not take into account the anisotropy of the electron and hole effective masses at the L point, while the tight-binding calculations of Refs. 14 and 20 significantly underestimate the effective-mass anisotropy, so both approaches miss the strong $P_h^{\parallel}$-$P_h^{\perp}$ and $P_e^{\parallel}$-$P_e^{\perp}$ splittings.

Recently, two experimental results[9,14] have been interpreted as to provide *direct evidence* to model I. First, Wehrenberg and Guyot-Sionnest[9] observed concurrent bleaching of the first and second interband absorption peaks when "spectator" electron or holes were loaded into the NCs by electrochemical charge injection. They concluded that the second absorption peak must involve the S_h and S_e energy levels and must therefore originate from the S_h-P_e and P_h-S_e transitions. This argument is based on the assumption that the injected charges occupy the quantum-confined S_e and S_h states. Recent pseudopotential calculations,[26] however, have shown that the observed attenuation in the intensity of the second absorption peak in the presence of "spectator" charges does not imply that such peak arises from S_h-P_e or P_h-S_e transitions. For example, if some of the loaded electrons are trapped in surface states, which are ubiquitous in colloidal NCs, the ensuing electrostatic field leads to a significant attenuation of *all* the absorption peaks, including those that *do not* involve S_h or S_e states. Thus, the reported bleaching of the second absorption peak upon charge injection does not unambiguously reveal the origin of the underlying transitions.

Second, Peterson *et al.*[14] measured the two-photon photoluminescence-excitation (2PPLE) spectra of PbSe NCs. They observed a broad 2PPLE peak that occurs at energies close to (~40 meV above) the second one-photon absorption peak. Since the two-photon selection rules are such that the observed 2PPLE peak must originate from S_h-P_e or P_h-S_e interband transitions, the authors suggested that such transitions are also responsible for the second one-photon absorp-

 ©2009 The American Physical Society

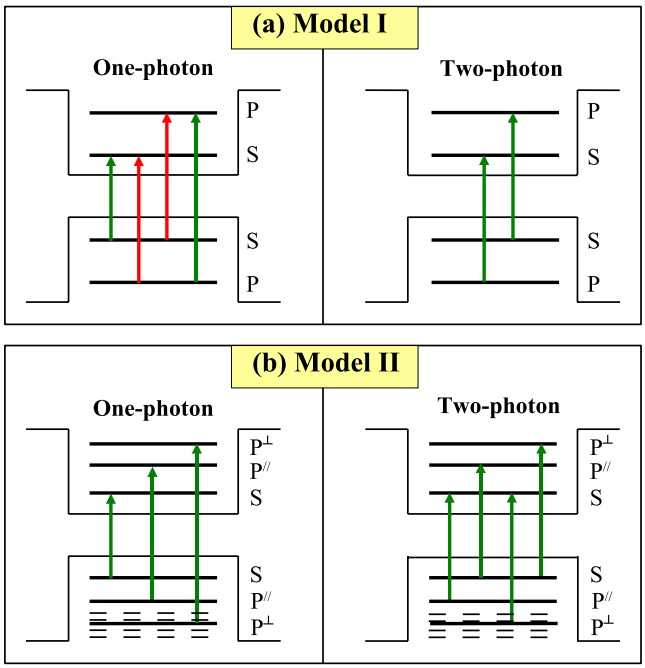

FIG. 1. (Color online) Schematic diagrams of the energy levels (horizontal lines) and interband optical transitions (vertical arrows) involved in the one-photon and two-photon absorption spectra of PbSe NCs, according to the two models that are prevalent in the literature. Green/light gray vertical arrows denote dipole-allowed interband transitions; red/gray vertical arrows denote dipole-forbidden transitions. Dashed horizontal lines indicate levels that do not contribute to the interband transitions.

tion peak.[14] As in previous studies favoring this interpretation,[2,3,10,17,21] the existence of intravalley splitting ($P^{\parallel}$ vs $P^{\perp}$) of the electron and hole P levels was ignored. What is needed is a calculation of one-photon and two-photon absorption spectra that include the $P^{\parallel}$-$P^{\perp}$ splitting, as well as other effects stemming from interband and intraband couplings.

We report here such a calculation using the atomistic pseudopotential method,[23,28] which includes effects missed in previous effective-mass calculations (e.g., intervalley and interband couplings, effective-mass anisotropy, and finite confinement barrier) or previous tight-binding calculations (e.g., correct rendering of the L-point effective-mass anisotropy). The calculated one-photon and two-photon absorption spectra are both in excellent agreement with the experimental results of Peterson *et al.*[14] We find that the *two-photon* absorption peaks originate from S_h-P_e and P_h-S_e transitions, as suggested in Ref. 14, while the second *one-photon* absorption peak originates from dipole-allowed $P_h^{\parallel}$-$P_e^{\parallel}$ transitions, not from dipole-forbidden S_h-P_e and S_h-P_e transitions as suggested in Ref. 14. We conclude that the correct model of the electronic structure of PbSe NCs is model II [Fig. 1(b)].

The calculations were performed using the semiempirical pseudopotential method described in Ref. 23. In this approach, we solve the single-particle Schrödinger equation

TABLE I. Calculated band-edge energy levels of a PbSe NC of radius R=30.6 Å, with respect to the S_h energy level.

Hole levels	Energy (eV)	Electron levels	Energy (eV)
S_h	0.00	S_e	0.89
$P_h^{\parallel}$	−0.09	$P_e^{\parallel}$	1.03
$P_h^{\perp}$	−0.23	$P_e^{\perp}$	1.16

$$\left[-\frac{\hbar^2}{2m}\nabla^2 + V(\boldsymbol{r}) + \hat{V}_{\mathrm{SO}}\right]\psi_i(\boldsymbol{r},\sigma) = \varepsilon_i\psi_i(\boldsymbol{r},\sigma), \tag{1}$$

where m is the bare electron mass, $\hat{V}_{\mathrm{SO}}$ is the spin-orbit operator, and $V(\boldsymbol{r})$ is the local pseudopotential, given by the superposition of screened atomic pseudopotentials v_n centered at the atomic positions $\{\boldsymbol{R}_n\}$,

$$V(\boldsymbol{r}) = \sum_n v_n(|\boldsymbol{r} - \boldsymbol{R}_n|). \tag{2}$$

The atomic pseudopotentials v_n and the spin-orbit operator $\hat{V}_{\mathrm{SO}}$ were fitted to experimental bulk transition energies, fully anisotropic L-point effective masses, and deformation potentials. The parameters of the Pb and Se pseudopotentials are given in Ref. 23. Equation (1) was solved by expanding the wave functions $\psi_i(\boldsymbol{r},\sigma)$ in a plane-wave basis set and by calculating the band-edge states using the folded-spectrum method.[29] Since the atomic pseudopotentials of Eq. (2) are screened, we were able to use a relatively small energy cutoff of 6 Ryd in the plane-wave expansion. The pseudopotential method includes intervalley coupling and intraband coupling, which are brought about in NCs by the lack of translational symmetry.

We consider a PbSe quasispherical NC of radius R =30.6 Å. The NC was constructed by cutting out a spherical segment from bulk PbSe (rock-salt lattice structure; lattice constant a_0=6.12 Å). The Pb and Se atoms at the surface of the NC were passivated using ligandlike potentials designed to remove surface states from the band gap.[23] While impurities may be present in the NCs, and may affect the emission spectrum, the *absorption* spectrum is dominated by intrinsic band-to-band transitions. Thus, the effects of impurities are negligible and are not included in the present calculations. The band-edge energy levels [schematically shown in Fig. 1(b)] are summarized in Table I. The calculated single-particle band gap (not including excitonic effects) is 0.89 eV. The band-edge states (S_h and S_e) have an S-like envelope function and are fourfold degenerate (eightfold degenerate including spin) because they originate from the fourfold-degenerate L points of the bulk PbSe Brillouin zone.[23,30] This degeneracy is lifted by intervalley coupling, but the resulting splitting is relatively small [~15 meV (Ref. 24)]. The S_e electron states are followed at higher energy by the fourfold-degenerate $P_e^{\parallel}$ states and the eightfold degenerate $P_e^{\perp}$ states. The S_e-$P_e^{\parallel}$ average energy separation is 0.14 eV, and the $P_e^{\parallel}$-$P_e^{\perp}$ separation is 0.13 eV. Similarly, the S_h hole states are followed at lower energy by the fourfold-degenerate $P_h^{\parallel}$

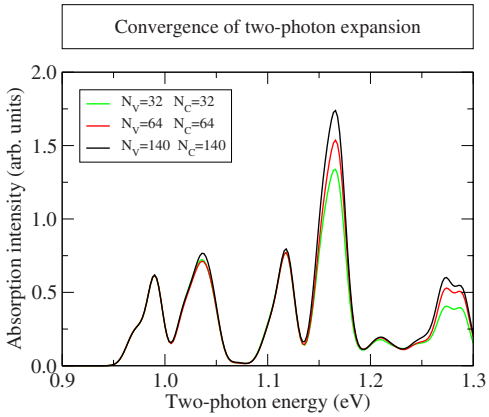

FIG. 2. (Color online) Convergence of the calculated two-photon absorption spectrum of a $R=30.6$ Å PbSe NC with the number of intermediate states included in the sum of Eq. (3).

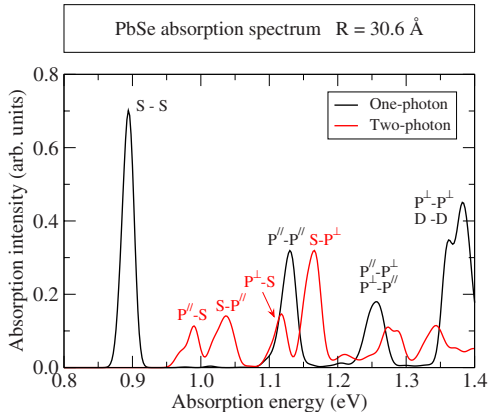

FIG. 3. (Color online) Calculated one-photon (black solid line) and two-photon (red/gray solid line) absorption spectra of a PbSe NC of radius $R=30.6$ Å. The transitions were broadened by a 10 meV Gaussian convolution function. The two-photon absorption intensity was rescaled to facilitate a comparison with the one-photon spectrum. Excitonic effects were not included.

states and the eightfold degenerate $P_h^\perp$ states (which have a significant D_h component[23]). The S_h-$P_h^\parallel$ average energy separation is 0.09 eV, and the $P_h^\parallel$-$P_h^\perp$ separation is 0.14 eV.

The one-photon absorption spectrum was calculated in the independent-particle approximation using Fermi's golden rule,

$$I_{1\text{-ph}}(\omega) \propto \sum_{v,c} |\langle \psi_v | \hat{\mathbf{r}} | \psi_c \rangle|^2 \delta(\varepsilon_c - \varepsilon_v - \hbar\omega), \tag{3}$$

where the sum runs over the valence (v) and conduction (c) states of the NC. Previous calculations[24] have shown that excitonic effects are relatively small in PbSe NCs because the large dielectric constant ($\varepsilon_\infty=23$) effectively screens electron-hole Coulomb interactions [exciton binding energy <40 meV for a 30.6 Å-radius PbSe NC (Ref. 24)]. Therefore, excitonic effects were not included in the calculation of the absorption spectrum.

The two-photon absorption spectrum was calculated from second-order perturbation theory as

$$I_{2\text{-ph}}(\omega) \propto \sum_{v,c} \sum_{\alpha} \left| \sum_i \frac{\langle \psi_c | r_\alpha | \psi_i \rangle \langle \psi_i | r_\alpha | \psi_v \rangle}{\varepsilon_i - \varepsilon_v - \hbar\omega} \right|^2 \times \delta(\varepsilon_c - \varepsilon_v - 2\hbar\omega), \tag{4}$$

where the first sum runs over the valence and conduction states (as in the case of the one-photon absorption spectrum), the second sum runs over the Cartesian coordinate indexes α, and the third sum runs over the intermediate states i (which can be either hole or electron states). We included up to 140 hole levels and 140 electron levels in the intermediate-state sum of Eq. (4). The convergence of the two-photon absorption spectrum is examined in Fig. 2, which shows $I_{2\text{-ph}}(\omega)$ as a function of the number of hole states (N_V) and electron states (N_C) retained in the sum over the intermediate states. We see that the first three peaks (whose origin will be discussed below) converge quickly as N_V and N_C are increased. The fourth and fifth peaks (at energies $\sim$1.17 and $\sim$1.28 eV, respectively) converge more slowly, and their intensity tends to increase as N_V and N_C increase.

The converged one-photon and two-photon absorption spectra of a $R=30.6$ Å PbSe NC are compared in Fig. 3. A detailed analysis of the origin of the one-photon absorption peaks was presented in Ref. 23. The one-photon spectrum (Fig. 3) exhibits four main peaks in an energy interval of $\sim$0.5 eV above the absorption edge. The first peak (centered at 0.89 eV) originates from S_h-S_e interband transitions. The second peak (at 1.13 eV) corresponds to $P_h^\parallel$-$P_e^\parallel$ transitions. The peak at 1.25 eV originates from weakly allowed $P_h^\parallel$-$P_e^\perp$ and $P_h^\perp$-$P_e^\parallel$ transitions. This peak has not been resolved experimentally presumably because it is masked by inhomogeneous broadening effects.[23] Finally, the peak at 1.38 eV originates from $P_h^\perp$-$P_e^\perp$ and D_h-D_e interband transitions. This peak corresponds to the third absorption peak observed in experiment.

The two-photon absorption spectrum (Fig. 3) exhibits four main peaks in the energy interval of 0.9–1.2 eV. We assign these four peaks to the (i) $P_h^\parallel$-S_e, (ii) S_h-$P_e^\parallel$, (iii) $P_h^\perp$-S_e, and (iv) S_h-$P_e^\perp$ two-photon transitions, as shown schematically in Fig. 1(b). The first ($P_h^\parallel$-S_e), second (S_h-$P_e^\parallel$), and third ($P_h^\perp$-S_e) peaks, located at 0.99, 1.03, and 1.12 eV, respectively, are relatively weak compared to the fourth (S_h-$P_e^\perp$) peak, centered at 1.17 eV. The splitting between the four peaks is due to (i) the L-point electron and hole effective-mass anisotropy, which splits the $P_e^\parallel$ states from the $P_e^\perp$ states and the $P_h^\parallel$ states from the $P_e^\perp$ states, and (ii) the slightly different effective masses of the electron and the hole, which is responsible for the difference between the $P_h^\parallel$-S_e and the S_h-$P_e^\parallel$ transitions (see Table I). It is very important to note that in our calculation the dominant S_h-$P_e^\perp$ two-photon peak is *higher* in energy than the second one-photon absorption peak ($P_h^\parallel$-$P_e^\parallel$). The fact that a S_h-P_e transition could be higher in energy than a P_h-P_e transition may appear counterintuitive. The reason for this apparent anomaly is that the $P_e^\perp$-$P_e^\parallel$ energy difference is larger than the S_h-$P_h^\parallel$ energy difference (see Table I).

Having established the origin of the one-photon and two-photon absorption peaks, we now compare our results with the experimental results of Peterson *et al.*[14] The authors measured the 2PPLE spectra of PbSe NCs ranging in diameter from 3 to 5 nm. They observed a broad 2PPLE peak, whose

width increases with decreasing NC size. This peak was attributed, based on a comparison with tight-binding calculations, to the two-photon-allowed S_h-P_e and P_h-S_e transitions. Our pseudopotential calculations predict four peaks in the two-photon absorption spectrum of $R=30.6$ Å PbSe NCs (Fig. 3). Since these peaks are close in energy, they are probably not resolved in the experiment of Ref. 14. Peterson *et al.*[14] also observed that the first 2PPLE peak is only slightly higher in energy than the second one-photon absorption peak, with the energy difference being 39 ± 12 meV. Thus, they concluded that the second one-photon absorption peak should also be assigned to S_h-P_e and P_h-S_e transitions. Since those transitions are dipole forbidden in one-photon absorption, the authors[14] suggested that some yet unexplored mechanisms could render those transitions allowed in the measured one-photon absorption spectrum. Our calculations also show a good match between the two-photon absorption peaks and the second one-photon absorption peak (see Fig. 3). The dominant two-photon peak, which we assign to the S_h-$P_e^{\perp}$ transition, is 36 meV higher in energy than the second one-photon peak, in excellent agreement with experiment. However, our pseudopotential calculations indicate that the second one-photon absorption peak originates from dipole-allowed P_h-P_e transitions (see Fig. 3), thereby obviating the need to go beyond the dipole approximation to explain the one-photon absorption spectrum.

Trapping of charges near the surface of a PbSe NC produces an electrostatic field inside the NC that can change the oscillator strength of the optical transitions. A similar effect can be expected if the NC has a ground-state dipole moment induced, for example, by irregular surface termination. Previous atomistic pseudopotential calculations[26] have shown that in the presence of a localized surface charge the oscillator strength of the S_h-S_e and P_h-P_e interband transitions decreases, while the formally forbidden S_h-P_e and P_h-S_e transitions acquire some oscillator strength. Due to the large dielectric constant of PbSe, however, any internal electric field is bound to be highly screened. As a result, the intensity of the S_h-P_e and P_h-S_e transitions is very weak.[26] Interestingly, CdSe NCs, which are believed to have a permanent ground-state dipole moment,[31] do not show appreciable S-P interband transitions in the one-photon absorption spectrum.[32] Furthermore, our calculations[26] show that the S_h-P_e and P_h-S_e transitions in PbSe NCs occur at significantly lower energy than the experimentally observed second absorption peak. Thus, we conclude that the conventional model of the electronic structure of PbSe NCs [Fig. 1(a)] is incorrect. Our results support instead the assignment of the one-photon and two-photon transitions given in Fig. 1(b).

This work was funded by the U.S. DOE, SC, BES, under Contract No. DE-AC36-08GO28308 to NREL.

[1] A. Luque, A. Martí, and A. J. Nozik, MRS Bull. **32**, 236 (2007).
[2] R. D. Schaller and V. I. Klimov, Phys. Rev. Lett. **92**, 186601 (2004).
[3] R. J. Ellingson *et al.*, Nano Lett. **5**, 865 (2005).
[4] B. L. Wehrenberg, C. Wang, and P. Guyot-Sionnest, J. Phys. Chem. B **106**, 10634 (2002).
[5] J. M. Pietryga *et al.*, J. Am. Chem. Soc. **126**, 11752 (2004).
[6] P. Liljeroth, P. A. Zeijlmans van Emmichoven, S. G. Hickey, H. Weller, B. Grandidier, G. Allan, and D. Vanmaekelbergh, Phys. Rev. Lett. **95**, 086801 (2005).
[7] A. Olkhovets, R. C. Hsu, A. Lipovskii, and F. W. Wise, Phys. Rev. Lett. **81**, 3539 (1998).
[8] H. Du, C. Chen, R. Krishnan, T. D. Krauss, J. M. Harbold, F. W. Wise, M. G. Thomas, and J. Silcox, Nano Lett. **2**, 1321 (2002).
[9] B. L. Wehrenberg and P. Guyot-Sionnest, J. Am. Chem. Soc. **125**, 7806 (2003).
[10] J. M. Harbold, H. Du, T. D. Krauss, K. S. Cho, C. B. Murray, and F. W. Wise, Phys. Rev. B **72**, 195312 (2005).
[11] R. D. Schaller, J. M. Pietryga, S. V. Goupalov, M. A. Petruska, S. A. Ivanov, and V. I. Klimov, Phys. Rev. Lett. **95**, 196401 (2005).
[12] J. M. Harbold and F. W. Wise, Phys. Rev. B **76**, 125304 (2007).
[13] C. Bonati, A. Cannizzo, D. Tonti, A. Tortschanoff, F. van Mourik, and M. Chergui, Phys. Rev. B **76**, 033304 (2007).
[14] J. J. Peterson, L. Huang, C. Delerue, G. Allan, and T. D. Krauss, Nano Lett. **7**, 3827 (2007).
[15] R. Koole, G. Allan, C. Delerue, A. Meijerink, D. Vanmaekelbergh, and A. J. Houtepen, Small **4**, 127 (2008).
[16] M. Tuan Trinh, A. J. Houtepen, J. M. Schins, J. Piris, and L. D. A. Siebbeles, Nano Lett. **8**, 2112 (2008).
[17] I. Kang and F. W. Wise, J. Opt. Soc. Am. B **14**, 1632 (1997).
[18] A. D. Andreev and A. A. Lipovskii, Phys. Rev. B **59**, 15402 (1999).
[19] G. E. Tudury, M. V. Marquezini, L. G. Ferreira, L. C. Barbosa, and C. L. Cesar, Phys. Rev. B **62**, 7357 (2000).
[20] G. Allan and C. Delerue, Phys. Rev. B **70**, 245321 (2004).
[21] A. Shabaev, Al. L. Efros, and A. J. Nozik, Nano Lett. **6**, 2856 (2006).
[22] A. Franceschetti, J. M. An, and A. Zunger, Nano Lett. **6**, 2191 (2006).
[23] J. M. An, A. Franceschetti, S. V. Dudiy, and A. Zunger, Nano Lett. **6**, 2728 (2006).
[24] J. M. An, A. Franceschetti, and A. Zunger, Nano Lett. **7**, 2129 (2007).
[25] J. M. An, A. Franceschetti, and A. Zunger, Phys. Rev. B **76**, 045401 (2007).
[26] J. M. An, A. Franceschetti, and A. Zunger, Phys. Rev. B **76**, 161310(R) (2007).
[27] J. M. An, M. Califano, A. Franceschetti, and A. Zunger, J. Chem. Phys. **128**, 164720 (2008).
[28] A. Franceschetti, H. Fu, L. W. Wang, and A. Zunger, Phys. Rev. B **60**, 1819 (1999).
[29] L. W. Wang and A. Zunger, J. Chem. Phys. **100**, 2394 (1994).
[30] S. H. Wei and A. Zunger, Phys. Rev. B **55**, 13605 (1997).
[31] S. A. Blanton, R. L. Leheny, M. A. Hines, and P. Guyot-Sionnest, Phys. Rev. Lett. **79**, 865 (1997).
[32] D. J. Norris and M. G. Bawendi, Phys. Rev. B **53**, 16338 (1996).